$M2$ Isomerism in ^{83}Rb and High-Resolution Spectroscopic Investigations of the Decay of ^{83}Sr

R. C. ETHERTON*†
Department of Physics, Michigan State University, East Lansing, Michigan
and
Department of Physics and Astronomy, Southern Illinois University, Carbondale, Illinois

AND

L. M. BEYER*† AND W. H. KELLY*
Department of Physics, Michigan State University, East Lansing, Michigan

AND

D. J. HOREN
U. S. Naval Radiological Defense Laboratory, San Francisco, California‡
(Received 17 August 1967)

The photon spectrum accompanying the electron-capture decay of ^{83}Sr has been studied with high-resolution Ge(Li) spectrometers in singles and coincidence configurations. The positron and internal-conversion-electron spectra were investigated with the MSU "orange" and $\pi\sqrt{2}$ iron-free electron spectrometers. Sixty transitions were identified. Excited states have been placed in ^{83}Rb at 5.0, 42.3, 295.2, 389.2, 423.5, 736.8, 804.8, 994.2, 1043.7, 1053.7, 1103.0, 1202.0, 1242.6, 1273.1, 1324.6, 1653.1, 1756.9, 1783.5, 1916.7, 1952.2, 2014.8, 2090.0, 2147.8, and 2179.3 keV. Internal-conversion coefficients, logft, and γ-ray branching ratios have been used to place limits upon the spins and parities of the excited states. An isomeric $M2$ transition of 42.3 keV has been identified. The ground-state spin and parity of ^{83}Sr have been shown to be $\frac{7}{2}^+$, which are the same as for all other known 45-neutron nuclei.

1. INTRODUCTION

USING shell-model configurations with the assumption that the nuclear potential is due to two-body effective interactions between nucleons, Talmi and Unna have made calculations[1] to predict the characters of the ground and first excited states of several strontium isotopes. At the same time, these authors noted the lack of experimental data for isotopes in this mass region. The present work was motivated by a desire to extend the data, as well as to test some of the results of their calculations for ^{83}Sr.

When this investigation was first started only three γ transitions of 40, 385, and 755 keV had been identified[2] as belonging to the decay of ^{83}Sr. Preliminary investigations by Maxia, Kelly, and Horen[3] have indicated that the decay of ^{83}Sr is somewhat more complex with observed transitions of 40, 375, 408, 770, 1160, 1560, and 1960 keV. Later, Reddy, Johnston, and Jha[4] presented data in agreement with Maxia *et al.* and placed levels at 40, 380, 480, 1160, 1560, 1960, and 2120 keV for ^{83}Rb. These data were all recorded with NaI(Tl) detectors.

It was soon evident from our early γ-γ coincidence data taken with NaI(Tl) detectors that the decay scheme was much more complex. We have used high-resolution Ge(Li) detectors in singles and coincidence configurations in order to perform a more complete investigation. Some 60 transitions have been identified as belonging to ^{83}Sr decay and have been fitted into a complex decay scheme. In addition, intermediate and high-resolution magnetic spectrometers have been used to measure the internal-conversion coefficients of several transitions, thus leading to additional information on the spin-parity assignments of the low-energy levels.

2. EXPERIMENTAL PROCEDURES

A. Source Preparation

The strontium-83 activity was produced from stable isotopes by means of two different nuclear reactions. The early γ-ray measurements were made using sources produced by bombarding arsenic metal with 10.4-MeV/nucleon ^{12}C ions in the Lawrence Radiation Laboratory HILAC when two of the present authors (DJH and WHK) were guests of LRL. Later sources were produced by bombarding rubidium chloride with 37- to 42-MeV protons from the Michigan State University cyclotron.

In both cases the strontium activities were separated chemically by precipitating the strontium with $SrCl_2$ carrier in chilled fuming nitric acid. Small amounts of ^{82}Sr and ^{85}Sr were present in the sources from the HILAC bombardment, whereas only the ^{85}Sr contaminant was present in the sources prepared with the cyclotron bombardments.

Two carrier-free chemical procedures were used to prepare the electron sources, all of which were cyclotron-

* Supported in part by the U. S. National Science Foundation.
† Present address: Department of Physics and Astronomy, Murray State University, Murray, Ky.
‡ Supported in part by U. S. Navy Bureau of Ships.
[1] I. Talmi and I. Unna, Nucl. Phys. **19**, 225 (1960).
[2] T. Kuroyanagi, J. Phys. Soc. Japan **16**, 2363 (1961).
[3] V. Maxia, W. H. Kelly, and D. J. Horen, J. Inorg. Nucl. Chem. **24**, 1175 (1962).
[4] K. R. Reddy, A. S. Johnston, and S. Jha, Bull. Am. Phys. Soc. **9**, 17 (1964); and private communication.

produced. The first technique[5] involved a coprecipitation of the strontium fraction with barium in chilled fuming nitric acid. The barium was then separated from the strontium by saturating a chilled 0.1 N HCl solution with HCl gas and precipitating only the barium.

The second carrier-free procedure involved a slightly modified version of the extraction technique originally reported by Kiba and Mizukani.[6] The RbCl target was dissolved in a few milliliters of a 0.5M buffer solution composed of acetic acid and ammonium hydroxide, adjusted to pH 8. The solution was transferred to a separatory funnel containing an equal volume of 0.05M TTA in hexone and extracted. After two extractions, the organic solution was found to contain about 90% of the ^{83}Sr produced, which was radiochemically free of rubidium activities. This solution was very convenient for the preparation of γ sources. The electron sources were obtained by back extraction of the strontium with a very small amount of 0.2N HNO_3. The procedure was simple, could be performed rapidly, and the purity of the sources produced appeared to be the same as those produced using the first technique.

The sources for the β-ray spectrometers were prepared from either of the above solutions by vacuum sublimation onto a 0.00025-cm aluminum foil. The $Sr(NO_3)_2$ proved to be more amenable to this technique than $SrCl_2$.

The ^{83}Sr γ spectra obtained from the sources produced using the heavy ion reactions appeared to be identical to those obtained from sources produced using the proton reactions.

B. Apparatus

The high-resolution γ-ray spectrometers consisted of Ge(Li) detectors[7] with sensitive volumes ranging from 1 to 7 cm^3. The associated electronics consisted of a low-noise vacuum tube or a field-effect transistor preamplifier and a low-noise RC pulse shaping amplifier coupled to a 1024-channel analyzer.

γ-γ coincidences were recorded using conventional fast-slow multiple coincidence circuits with resolving times of approximately 50 nsec. The γ detectors used for these experiments were the 7-cm^3 Ge(Li) and either a 7.6 by 7.6-cm NaI(Tl) or a split-annulus NaI(Tl) detector.[8]

The 7-cm^3 Ge(Li) and split-annulus NaI(Tl) detectors were used as an anti-Compton, a pair, and an any-coincidence spectrometer, as described in Ref. 8.

A large fraction of the conversion electron and positron data was recorded with the MSU "Orange" spectrometer.[9] The baffles and detector slit were set for a resolution of 0.8% at a transmission of approximately 5%. Most of the measurements on the 42.3-keV transition were recorded with the MSU iron-free $\pi\sqrt{2}$ spectrometer.[10] In these latter measurements, the baffles were set for a resolution of 0.2%. However, source thickness strongly limited the resolution of the low-energy lines.

3. EXPERIMENTAL RESULTS

A. γ-Ray Singles Spectrum

The γ-ray singles spectrum taken with a Ge(Li) detector of 3-cm^3 sensitive volume and resolution of 3 keV for the 662-keV ^{137}Cs photon is shown in Figs. 1(A) and 1(B). The low-energy part of the spectrum, taken with an expanded gain, is shown in Fig. 1(A), while the high-energy portion is shown in Fig. 1(B).

The energies of the observed photon transitions are listed in Table I along with their relative intensities. The energies of the more intense transitions were determined from spectra taken with ^{83}Sr sources mixed with photon emitters containing transitions of well-known energies.[11] These standard energies are listed in Table II. The technique used to determine the energy calibration curve was to least-squares-fit the peak centroids of the well-known transitions to a quadratic equation after the background had been subtracted from under the peaks. The background was obtained from a third-order least-squares fit to the counts in the channels adjacent to both sides of the peak. The deviations of the energies of the calibration transitions from the quadratic fit were never greater than $\pm$0.1 keV. The energies of the low-intensity photons were similarly determined using the strong transitions in ^{83}Sr as standards. The energies thus obtained were consistent at various gain settings. The RMS deviations from the average energies for the strong transitions listed in Table I ranged from $\pm$0.1 to $\pm$0.2 keV. The errors quoted in Table I include an estimate of $\pm$0.3 keV to account for any systematic errors that may have been present.

The relative intensities were obtained using experimentally determined efficiency curves.[12] For comparison, the relative intensities of the strong transitions measured with NaI(Tl) detectors are also listed in Table I. In general, the agreement of the two measurements was quite good.

Several very weak transitions were observed in spectra obtained using the anti-Compton spectrometer. These spectra were obtained from two different source geometries with respect to the Ge(Li) and NaI(Tl) split-annulus detectors, and are shown in Figs. 2(A) and 2(B).

[5] W. N. Sunderman and C. W. Townby, Natl. Acad. Sci.—Natl. Res. Council Publ. NAS–NS 3010 (1960).
[6] Ioshiyasu Kiba, and Ihigeru Mizukanii, Bull. Chem. Soc. Japan **31**, 1007 (1958).
[7] We are grateful to Dr. G. Berzins, who made these detectors, for help in their use.
[8] R. L. Auble *et al.*, Nucl. Instr. Methods **51**, 61 (1967).
[9] K. M. Bisgord, Nucl. Instr. Methods **22**, 221 (1963).
[10] L. J. Velinsky, Ph.D. thesis, Michigan State University, 1965 (unpublished); Q. L. Baird, J. C. Nall, S. K. Haynes, and J. H. Hamilton, Nucl. Instr. Methods **16**, 275 (1962).
[11] G. T. Ewan and A. J. Tavendale, Atomic Energy Commission, Limited (Canada) Report No. AECL2079, 1964 (unpublished) and references cited therein.
[12] R. L. Auble (private communication).

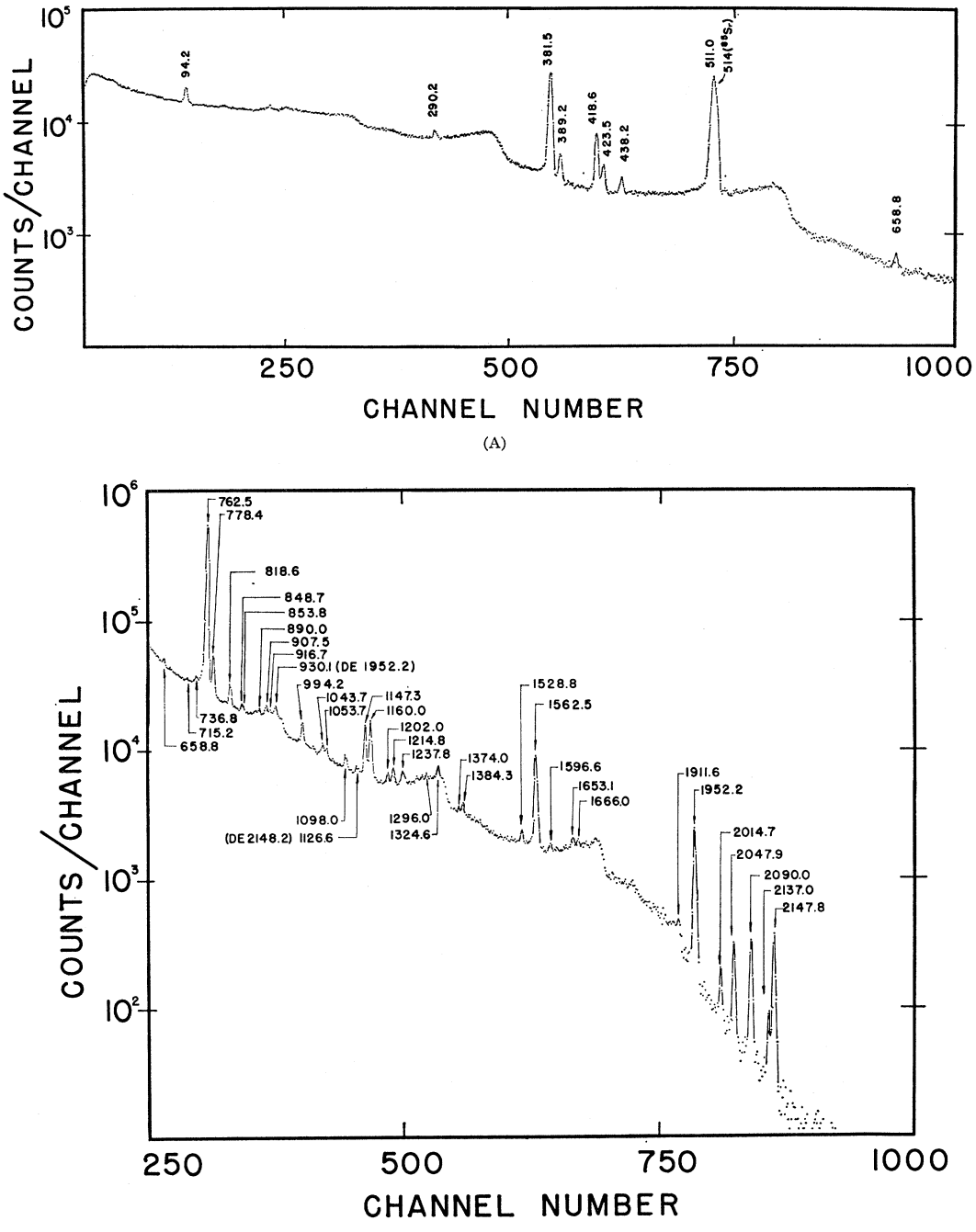

FIG. 1. Photon singles spectrum of ^{83}Sr taken with a 3-cm^3 Ge(Li) detector. (A) Low-energy region. (B) High-energy region.

In one case, the source was placed outside the annulus and the photons collimated into the Ge(Li) detector. In the second case, the source was inserted into the well of the annulus and a 5.1 by 5.1-cm NaI(Tl) detector was mounted in the tunnel above the source to increase the total solid angle subtended by the NaI(Tl) detectors. In this second case, more real coincidences due to γ cascades in the source were subtracted from the spectrum than in the first case. Therefore, in addition to improving peak to Compton ratios, those transitions involved in strong coincidence cascades can also be determined easily. The energies and relative intensities of the γ rays observed in these anti-Compton spectra are listed in Table III. These intensities are given rela-

TABLE I. Energies and relative intensities of transitions from the decay of ^{83}Sr.

Energy keV	Relative photon intensity[a] Ge(Li)	NaI(Tl)	Energy keV	Relative photon intensity[a] Ge(Li)	NaI(Tl)
(K x ray)		376.0	805 ±2.0[b]	0.1	
42.3±0.1[c]		5.2	818.6±0.5	2.4	
94.2±0.5	1.0	1.0	848.7±1.0	0.4	
290.2±0.5	1.4	1.2	853.8±0.5	0.4	
381.5±0.5[d]	60 }	53	889.0±0.5	0.4	
389.2±0.5	4.0 }		907.5±0.5	0.5	
418.6±0.5	17.8 }	18	916.7±1.0	0.1	
423.5±0.7	4.6 }		944.2±1.0	0.1	
438.2±0.5	2.7		994.2±0.5	1.5	
511.0[e]	163.2		1020 ±1.0[f]	0.1	
540.6±1.0	0.1		1036.8±1.0	0.2	
644.5±1.0	0.1		1043.7±1.0	0.5	
652.8±1.0	0.1		1053.7±0.7	0.6	
658.6±1.0	0.4		1098.0±0.5	0.6	
674.0±1.0	0.1		1147.3±0.5	3.8 }	7.8
714.2±1.0	0.2		1160.0±0.5	4.5 }	
732.0±1.0	0.2		1202.0±0.5	0.4	
736.8±0.5	0.5		1214.8±0.5	0.4	
753 ±2.0[f]	0.1 }		1237.6±1.0	0.5	
762.5±0.5	≡100 }	≡100	1242.6±1.0	0.3	
778.4±0.5	5.5 }		1273.1±1.0	0.1	
1284.6±1.0	0.1		1757 ±2.0[b]	0.1	
1296.0±1.0	0.4		1778 ±2.0[b]	0.08	
1324.6±1.0	0.5		1796 ±2.0[b]	0.14	
1374.0±1.0	0.2		1874 ±2.0[b]	0.1	
1384.0±1.0[b]	0.5		1911.6±1.0	0.14	
1528.8±1.0	0.2		1947 ±1.0[b]	0.1 }	2.7
1562.5±0.5	5.5	4.5	1952.2±0.5	2.6 }	
1596 ±2.0[b]	0.1		2014.7±0.7	0.1	
1653.1±1.0	0.3		2047.9±0.7	0.3	
1666.0±1.0	0.1		2090.0±0.7	0.3	
1710 ±2.0[b]	0.3		2137.0±1.0	0.1	
1722 ±2.0[b]	0.2		2147.8±0.7	0.5	
1749 ±2.0[b]	0.1				

[a] A 10% error in relative intensities is estimated.
[b] Seen in anti-Compton spectra only.
[c] $\pi\sqrt{2}$ β-ray spectrometer measurement.
[d] Doublet.
[e] Annihilation quanta. Total relative intensity determined with total annihilation.
[f] Seen in coincidence spectra only.

tive to the intensity of the 1952.2-keV transition which, as will be seen later, is not in coincidence with any photons.

B. γ-γ Coincidence Studies

γ-γ coincidence experiments were performed for all of the strong transitions and many of the weak ones. Initially, these were made using two 7.6 by 7.6-cm NaI(Tl) scintillation detectors. The energy resolutions of these detectors were approximately 8% for the 662-keV photon of ^{137}Cs. Later, the coincidence experiments were repeated using either a 7.6 by 7.6-cm NaI(Tl) crystal or the split-annulus NaI(Tl) crystal

TABLE II. Calibration energies.[a]

Source	Energy, keV[b]
^{131}I	80.164
^{123m}Te	159.00
^{131}I	284.307
^{131}I	364.467
Annihilation	511.006
^{137}Cs	661.595
^{60}Co	1173.226
^{60}Co	1332.483
ThC″ (DE)	1592.46
^{88}Y	1836.2
ThC″	2614.47

[a] Reference 11.
[b] Errors in these energies are ≲0.1 keV except for ^{88}Y, which is ±0.3 keV.

TABLE III. Energies and relative intensities of photons in the decay of ^{83}Sr observed in the anti-Compton and "any γ-γ" coincidence experiments.

Energy keV	Relative intensity Anti-Compton Collimated[a]	Uncollimated[b]	Any γ-γ coincidence
290.2	1.1		
381.5	48.0	24.2	210
389.2	3.9	1.3	27.5
418.6	13.7	6.8	50.3
423.5	3.7	1.8	12.8
438.0	2.3	0.3	7.5
511.0			256
658.6	0.33		5.8
714.2	0.15		2.2
732.0	0.16		3.0
736.8	0.48	0.2	6.6
762.5	90.0	63.9	≡100
778.4	4.5	1.2	31.8
805		0.1	
818.6	1.8	0.67	15.5
848.7	0.34	0.1	5.5
853.8	0.44	0.2	2.6
889.2	0.38		3.5
907.5	0.57	0.29	11.4
916.7	0.24		8.8
944.2	0.55	0.1	6.8
994.2	1.3	0.43	12.5
1036.6	0.14	0.06	2.7
1043.7	0.86	0.37	6.8
1053.7	0.5	0.33	5.7
1098.0	0.63	0.22	4.0
1147.3	3.3	1.2	34.3
1160.0	3.9	3.9	3.2
1202.0	0.56	0.42	
1214.8	0.7	0.2	6.8
1237.6	0.46	0.45	
1242.6	0.26	0.29	
1296.0	0.3	0.4	3.5
1324.6	0.73	0.37	7.5
1374.0	0.20	0.04	
1384.0	0.57	0.14	5.4
1528.8	0.30	0.05	3.0
1562.5	5.0	1.7	39.3
1596		0.07	
1653.1	0.21	0.22	
1666.0	0.16	0.05	2.3
1710		0.26	
1722		0.18	
1749		0.10	
1757		0.10	
1778		0.08	
1796		0.14	
1874	0.05	0.08	
1911.6	0.14	0.14	
1947		0.1	
1952.2	≡2.6[c]	≡2.6[c]	
2014.7	0.11	0.14	
2047.9	0.34	0.31	
2090.0	0.41	0.37	
2137.0	0.11	0.09	
2147.8	0.57	0.55	

[a] Source outside annulus tunnel.
[b] Source inside annulus tunnel, immediately adjacent to the Ge(Li) detector.
[c] Adjusted to equal relative intensity of the 1952.2 photon in singles.

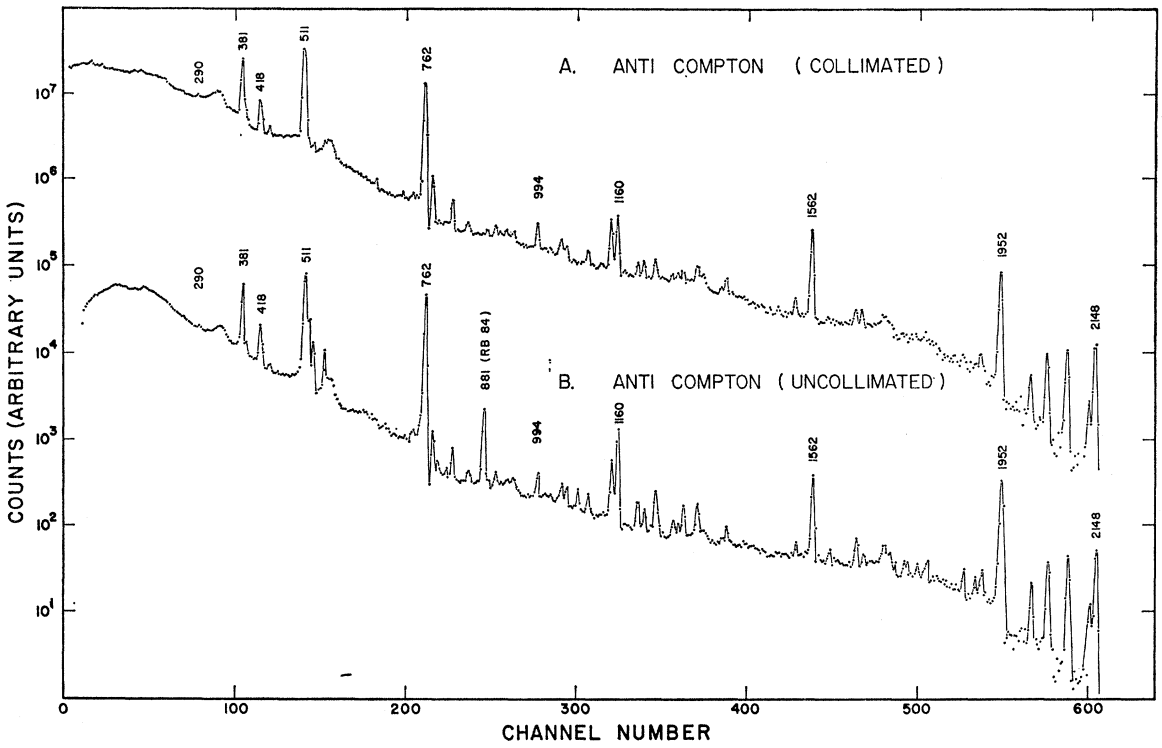

FIG. 2. Anti-Compton photon spectra of ^{83}Sr taken with a 7-cm^3 Ge(Li) and the split-annulus NaI(T1) detectors. Spectrum A was recorded with the source placed external to the annulus with the γ rays collimated into the Ge(Li). Spectrum B was recorded with the source placed adjacent to the Ge(Li) detector.

as the gate detector and a 7-cm^3 Ge(Li) detector for display on the 1024-channel analyzer. The energy resolution of the 7-cm^3 Ge(Li) detector was 4.5 keV for the 662-keV photon of ^{137}Cs. The results of both studies were consistent and only those data taken with the germanium detector will be discussed here.

In order to complement the anti-Compton data, a coincidence spectrum with the NaI(Tl) annulus–Ge(Li) system was recorded using an integral gate. This is called the "any γ-γ coincidence experiment." For this measurement, the source was sandwiched between 0.35 cm of copper to produce total annihilation and then placed 2 cm above the Ge(Li) detector. A 2.2-cm-thick cylindrical iron shield was placed around the Ge(Li) detector to reduce crystal-to-crystal scattering. The coincidence spectrum recorded from this con-

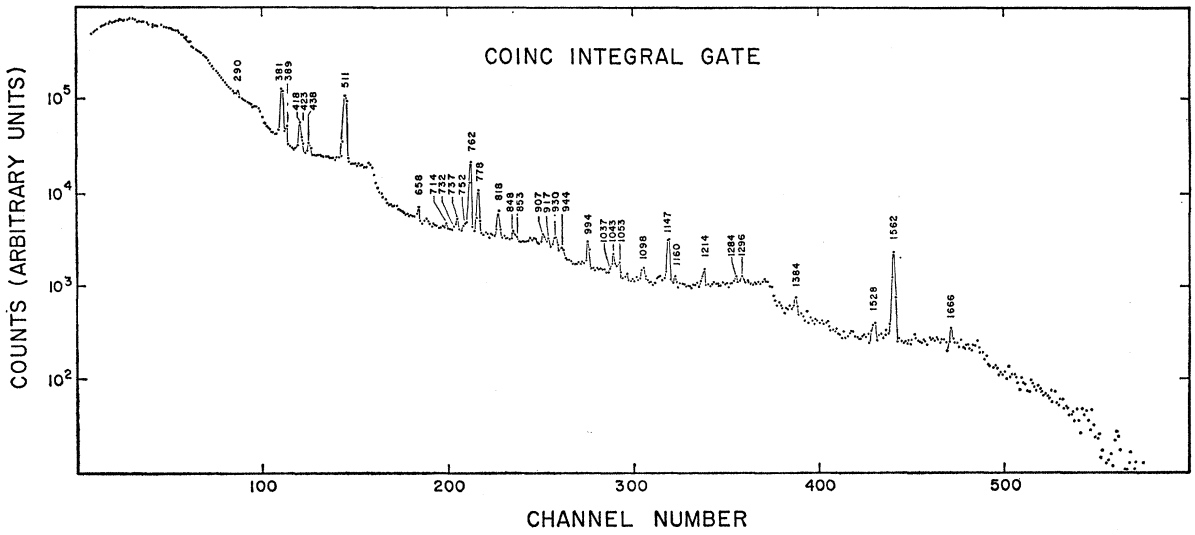

FIG. 3. "Any γ-γ coincidence" spectrum recorded with the 7-cm^3 Ge(Li) and split-annulus NaI(Tl) detectors.

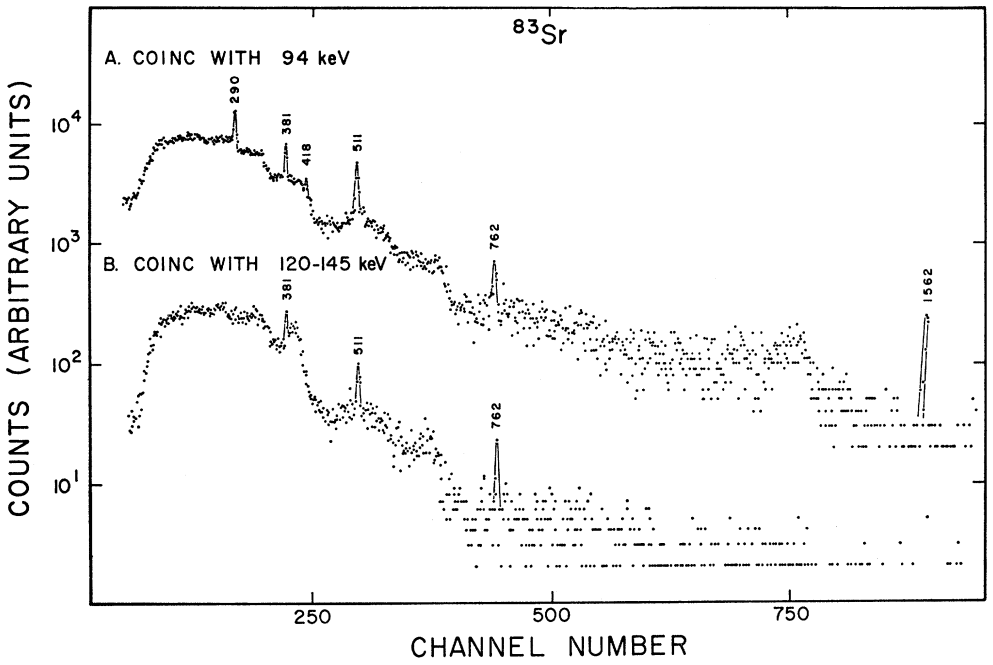

FIG. 4. Photon spectrum in coincidence with the 94.2-keV photon taken with the 7-cm^3 Ge(Li) detector. The coincidence gate detector was a 3.8 by 2.5-cm NaI(Tl) crystal with a 0.013-cm beryllium window. For comparison, spectrum B was recorded with the NaI(Tl) detector gating on the region above the 94.2-keV photon.

figuration is shown in Fig. 3. The energies and relative intensities of the photons observed in this coincidence spectrum are also listed in Table III. Almost all of the photons were noticeably enhanced relative to the 762.5-keV γ ray, indicating that this photon is not in as strong coincidence as many of the others.

Additional coincidence spectra were recorded in separate experiments with the coincidence gates set on

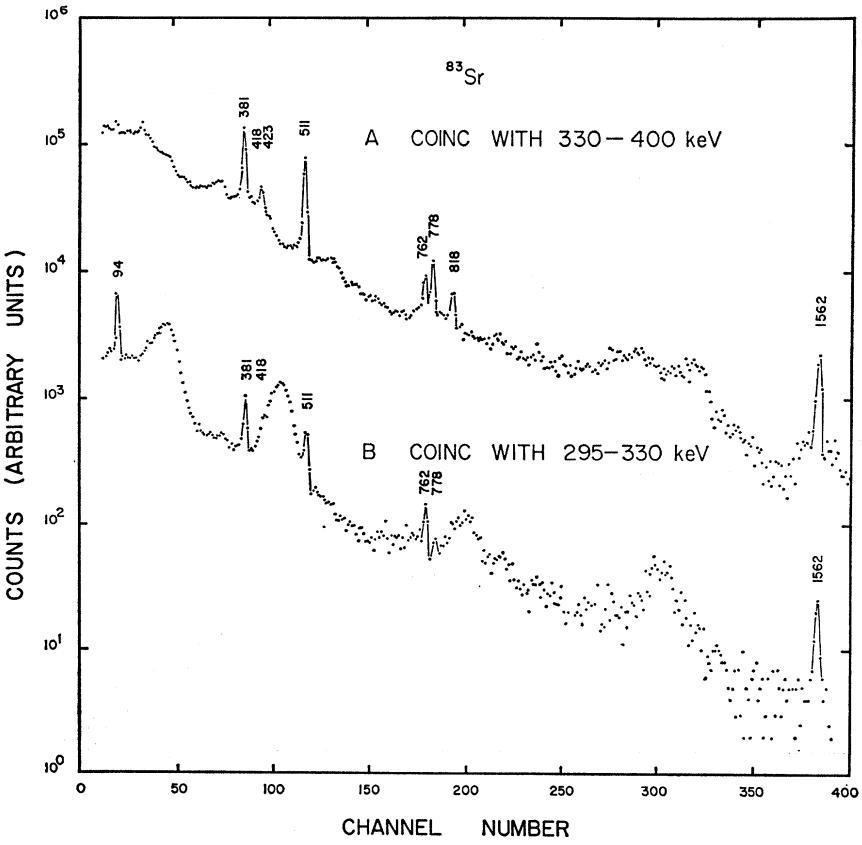

FIG. 5. Photon spectra in coincidence with segements of the 295–400-keV region taken with the 7-cm^3 Ge(Li) and 7.6 by 7.6-cm NaI(Tl) detectors. Spectrum B was recorded with the NaI(Tl) detector gated on 295–330 keV and includes part of the 290.2-keV photopeak. Spectrum A was recorded with the NaI(Tl) detector gated on the low-energy side of the 381-, 418-, and 423-keV photopeak.

the peaks with energies of 94.2, 381.5, 418.6, 762.5, 1147.3, 1160.0, and 1562.5 keV. For comparison, coincidence spectra were also recorded for coincidence gates set on the Compton regions below and above these peaks. Also, the 600–735-keV and 800–1100-keV regions of the spectrum were divided into six segments of 50- to 100-keV width and coincidence gates set on each segment.

Three different NaI(Tl) detectors were used to provide the coincidence gates. A 3.8 by 2.5-cm NaI(Tl) detector with a 0.013-cm beryllium window was used for the coincidence gates set on the 94.2-keV photopeak and the Compton region directly above it. A 7.6 by 7.6-cm NaI(Tl) detector was used for the coincidence gates set to the 381.5, 762.5, and 1562.5-keV photopeaks. The split-annulus NaI(Tl) detector was used for all of the other coincidence gates. The results of all these measurements are shown in Figs. 4–11, inclusive. Many of the spectra have been gain shifted by the computer for ease of comparison and presentation. These spectra have not been corrected for chance coincidences; however, the gross true-to-chance ratio was monitored and in every experiment it was 25 to 1 or greater.

In order to identify the states populated by positron decay, a triple coincidence experiment was performed using the NaI(Tl) split annulus and the 7-cm^3 Ge(Li) detectors. The source was placed into the well of the split annulus and immediately above the Ge(Li) detector. The pulses from each half of the split-annulus were used to provide a coincidence gate on the 511-keV photopeak. The coincidence spectrum recorded from this configuration is shown in Fig. 12(B). In order to distinguish those photons depopulating the states fed by the positron decay from the double escape peaks of the high-energy photons, the experiment was repeated

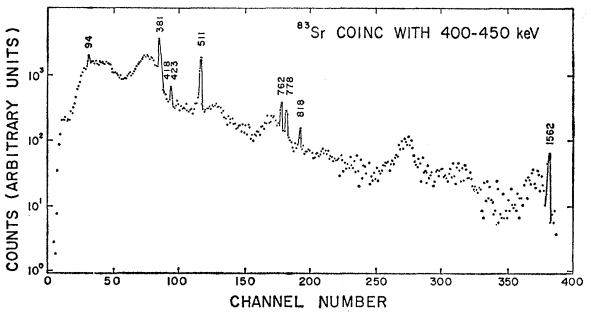

FIG. 6. Photon spectrum in coincidence with the 400–450-keV region taken with the 7-cm^3 Ge(Li) and the NaI(Tl) split-annulus detectors.

with the source placed external to the split-annulus detector and the photons collimated into the Ge(Li) detector. This spectrum, which contains only the double escape peaks, is shown in Fig. 12(C).

Note that the double escape peak of the 1562.5-keV photons was greatly reduced in the spectrum obtained with the source in the annulus [Fig. 12(B)]. This was caused by the 511-keV annihilation quanta from the 1562.5-keV photons summing with the coincident 94.2-, 290.2-, and 389.2-keV photons. These photons were very efficiently detected in the split annulus and the summing produced pulses corresponding to energies appreciably greater than 511 keV and therefore the gate requirement was no longer satisfied. The intensity of photons in cascades that are in coincidence with the positrons will be reduced similarly in the coincidence spectrum.

In almost every case, the coincidence gates necessarily included two or more γ rays because of their close energy spacings, and, in addition, many underlying Compton photons. This makes the interpretation of

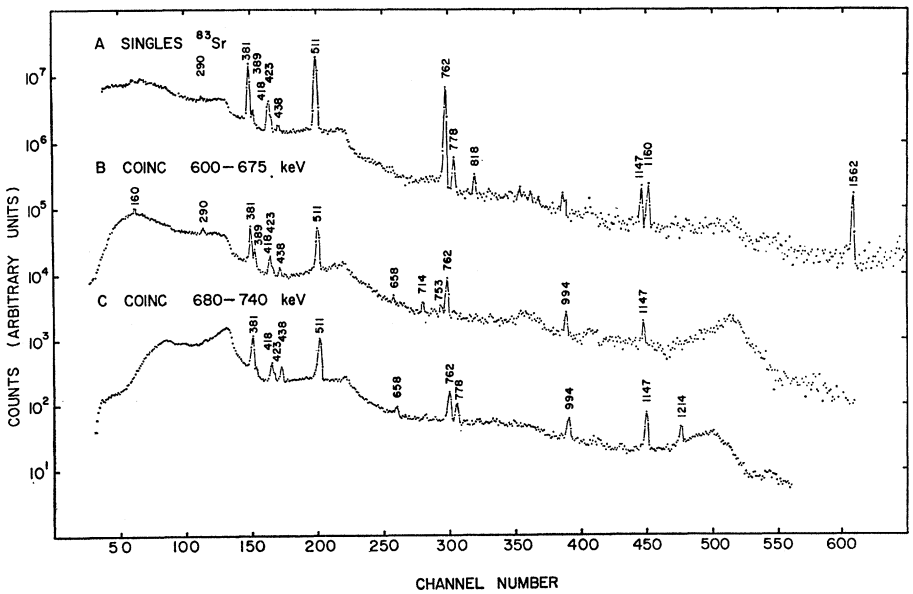

FIG. 7. Photon spectra in coincidence with segments of the 600–740-keV region taken with the same detection system as used for Fig. 6. A singles spectrum is given for reference. The spectra have been adjusted to have the same energy scales with the MSU CDC 3600 computer.

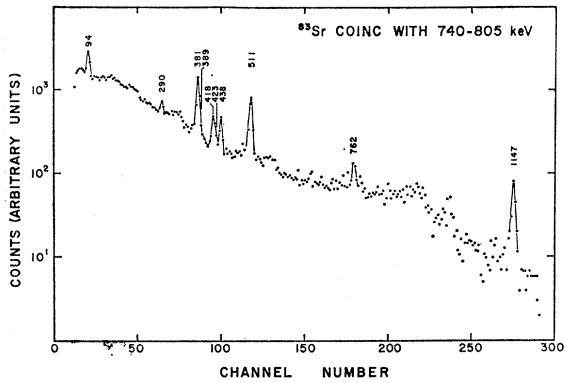

FIG. 8. Photon spectrum in coincidence with the 762.5-keV peak taken with the same detectors as used for Fig. 5.

most of the coincidence data difficult. However, a consistent interpretation can be obtained by quantitative comparisons of the different coincidence spectra. A summary of the coincidences seen in these experiments is presented in Table IV. It is possible to establish, by the comparison of spectra recorded with adjacent coincidence gates, that some of the peaks appearing in the coincidence spectra are the result of coincidences with Compton photons or sum peaks in the gate interval. These are listed in Table IV under the heading "Compton or sum coincidence". The appearance of the 511-keV peak in all of the coincidence spectra of the coincidence gates between 900–1200 keV can be accounted for by sum coincidences. These arise from one of the 511-keV annihilation quanta summing with any of the coincident 381.5-, 418.6-, 423.5- or 762.5-keV photons or their Compton photons in the NaI(Tl) annulus detector.

Comparisons of the coincidence spectra obtained from gates at 680–740 keV, 740–805 keV, 815–880 keV and 1100–1200 keV [Figs. 7(C), 8, 9(B), and 10] reveal that the 762.5-keV transition is in coincidence with the 1147.3-keV photons. Further, the peak at 438.2 keV is

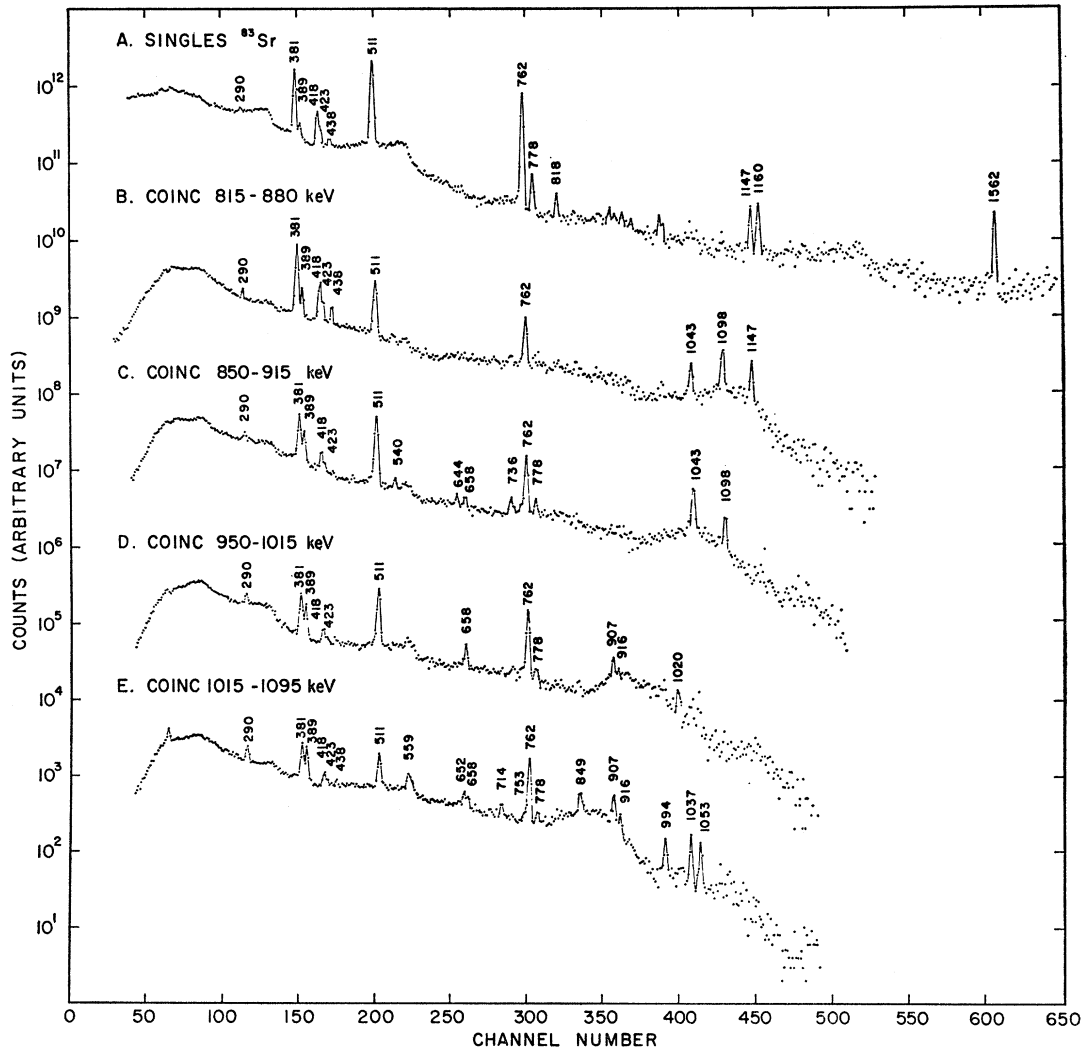

FIG. 9. Photon spectra in coincidence with various segments of the 800–1100-keV region. Spectrum A is a singles spectrum for reference. The detectors were the same as for Fig. 6. The energy scales have been adjusted as in Fig. 7.

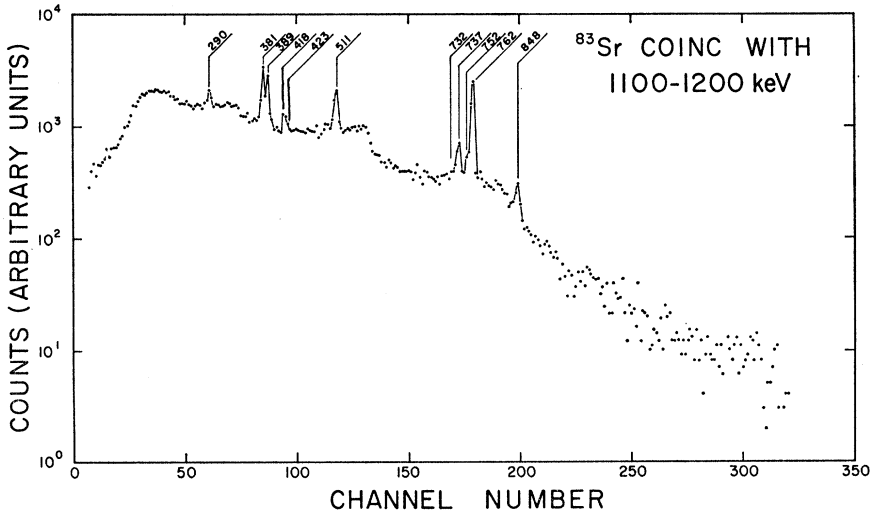

FIG. 10. Photon spectrum in coincidence with the 1147–1160-keV doublet. The detectors were the same as used for Fig. 5.

concluded to be in coincidence with the 762.5-keV γ, since the 762.5-keV peak is observed to grow as the coincidence gate is moved from 295–400 to 400–450 keV [Figs. 5(B), 5(A), and 6].

The ratio of the intensity of the 381.5-keV photon with the combined intensities of the 418.6- and 423.5-keV photons recorded in the coincidence spectra obtained with the coincidence gates at 330–400, 400–450, 740–805, and 1100–1200 keV [Figs. 5(A), 6, 8, and 10] are very informative and were crucial in the construction of the decay scheme. These ratios were 4.2, 5.2, 2.3, and 4.0, respectively, in comparison to 2.7 in the singles spectrum. Furthermore, the 418.6- and 423.5-keV photons always appeared in the coincidence spectra together and in the same intensity ratio as in singles. These ratios can be explained only with the conclusion that the 381.5-keV peak actually consists of two photons very close in energy, with one of them in coincidence with the other as well as with the 418.6- and 423.5-keV photons. The relative intensities of the two 381.5-keV photons have been calculated from the coincidence data to be 23.5 for the one in coincidence with the 418.6- and 423.5-keV photons and 36.5 for the other. No noticeable broadening of the 381.5-keV peak was observed. An upper limit of 0.2 keV is placed for the energy difference of the doublet.

The 42.3-keV transition was not observed to be in

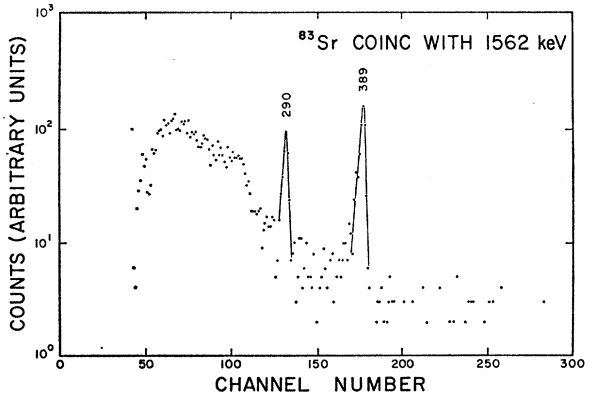

FIG. 11. Photon spectrum in coincidence with the 1562.5-keV peak. The detectors were the same as used for Fig. 5.

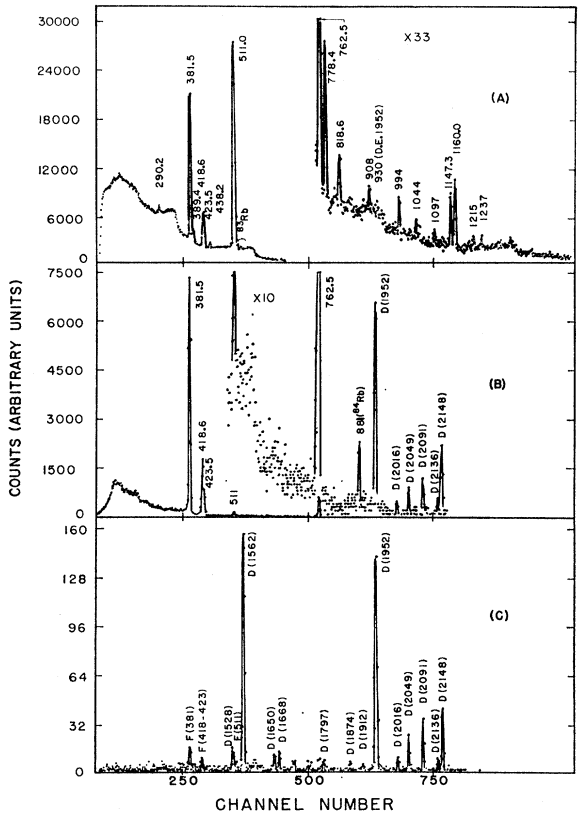

FIG. 12. Positron feeding spectra of ^{83}Sr taken with the same detectors as used for Fig. 6. Spectrum A is a singles spectrum which is shown for reference. Spectrum B is the positron feeding *and* double escape spectrum obtained with the γ rays collimated into the Ge(Li) detector from an external source. Spectrum C is the double-escape spectrum recorded with the pair spectrometer as described in Ref. 8.

TABLE IV. Coincidence summary.

Gate interval in keV	γ in gate in keV	Coincidence with γ in keV	Compton or sum coincidences	Figure No.
87–112	94.2	290.2, 1562.5	381.5, 418.6, 423.5, 511.0, 762.5	4(A)
120–145	None		381.5, 418.6, 423.5, 511.0, 762.5	4(B)
295–330	290.2	94.2, 1562.5	381.5, 418.6, 511.0, 762.5, 778.4	5(A)
340–400	381.5, 389.2, 418.6, 423.5	381.5, 418.6, 423.5, 511.0, 778.4, 818.6, 1562.5	94.2, 762.5	5(B)
400–450	381.5, 389.2, 418.6, 423.5, 438.2	381.5, 418.6, 423.5, 511.0, 762.5, 778.4, 818.6, 1562.5	94.2	6
600–675	644.5, 652.8, 658.6, 674.0	381.5, 418.6, 423.5, 658.6, 714.2, 753.2, 762.5, 994.2	290.2, 389.2, 511.0, 1147.3	7(B)
680–740	674.0, 714.2, 732.0, 736.8, 753.2, 762.5	381.5, 418.6, 423.5, 438.2, 511.0, 658.6, 714.2, 762.5, 778.4, 994.2, 1043.7, 1147.3, 1214.8		8
740–805	732.0, 736.8, 753.2, 762.5, 778.4, 818.6	381.5, 418.6, 423.5, 438.2, 511.0, 762.5, 778.4, 1147.3		8
815–880	818.6, 848.7, 853.8, 989.2	381.5, 418.6, 423.5, 438.2, 762.5, 1043.7, 1098.0, 1147.3	290.2, 389.2, 511.0	9(B)
850–915	848.7, 853.8, 889.2, 907.5 916.7	381.5, 418.6, 423.5, 540.2, 644.5, 658.6, 732.0, 736.8, 762.5, 778.4, 1043.7, 1098.0	290.2, 389.2, 511.0	9(C)
950–1015	944.2, 994.2, 1020.1	381.5, 418.6, 423.5, 658.6, 762.5, 778.4, 907.5, 994.2, 1020.1, 1053.7	290.2, 389.2, 511.0	9(D)
1015–1095	1020.1, 1037.8, 1043.7, 1053.7, 1098.0	381.5, 418.6, 423.5, 559, 652, 658, 714.2, 753.2, 762.5, 778.4, 848, 907.5, 916.7, 994.2, 1037.8, 1053.7	290.2, 389.2, 511.0	9(E)
1100–1200	1098.0, 1147.3, 1160.0, 1202.0, 1214.8	318.5, 418.6, 423.5, 732.0, 736.8, 753.2, 762.5, 848.7	290.2, 389.2, 511.0	10
1525–1600	1528.8, 1562.5	94.2, 290.2, 389.2		11

prompt coincidence with any of the other photons, x rays, or positrons.

C. Conversion Coefficients and the Positron Spectra

1. 42.3-keV Transition and the Search for an Isomer in ^{83}Sr

It is well known that the isotopes ^{87}Sr and ^{85}Sr possess isomeric states which arise from the filling of the $p_{1/2}$ and $g_{9/2}$ shells in this region. In addition, Talmi and Unna[1] predict a similar type structure for ^{83}Sr, suggestive of an isomeric state. From the lack of observed transitions in prompt coincidence with the 42.3-keV photon, a question arises as to whether this transition might be in the parent. In order to clarify this point, its K, L, and M conversion electron spectra were recorded with the $\pi\sqrt{2}$ β spectrometer and the results

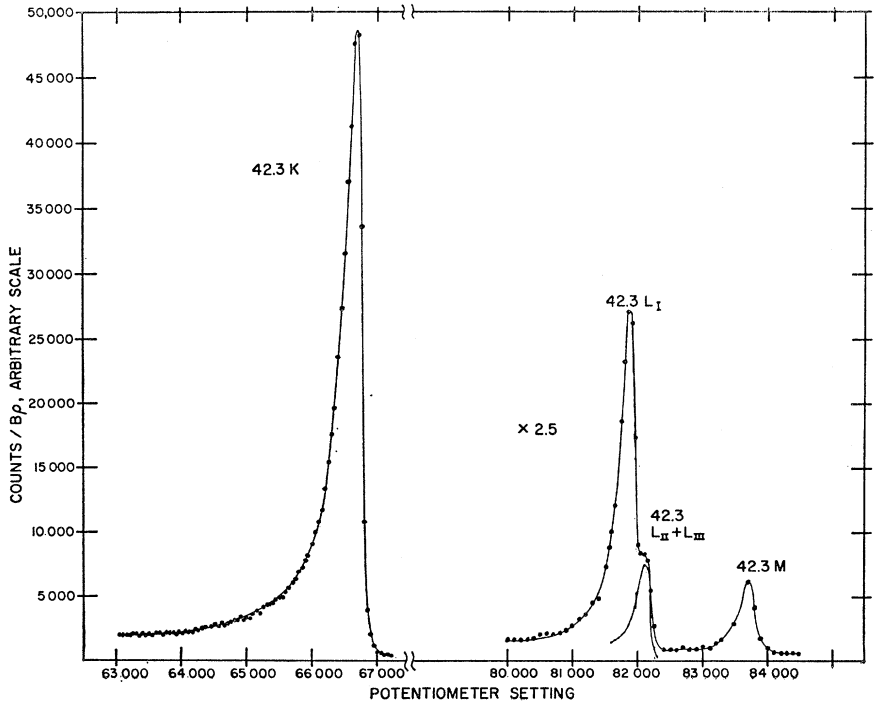

FIG. 13. The K, L, and M conversion electron lines of the 42.3-keV transition in ^{83}Rb. This spectrum was recorded with the MSU $\pi\sqrt{2}$ iron-free spectrometer.

TABLE V. Experimental results of the internal-conversion electron measurements on the 42.3-keV transition.

E_γ (keV)	$E_K-E_{L_I}$ (keV)	E_K-E_M (keV)	α_K	K/L	$L_I/(L_{II}+L_{III})$	K/M
42.3±0.05	13.20±0.03	15.0±0.1	29.3±3.5	5.5±0.1	2.8±0.2	30±2

are shown in Fig. 13. The measured K-L and K-M energy differences were compared with x-ray binding energies and were found to deviate by only 0.07 keV from the values for rubidium as is shown in Tables V and VI. Hence, we conclude the 42.3-keV transition is in rubidium. Several other experiments were performed to specifically search for an isomeric state in ^{83}Sr, but no positive evidence was found for the existence of the isomer. The fast chemical procedures described in Sec. 2A have been utilized to place an upper limit of 2 min on the half-life of any existing short-lived isomeric state in ^{83}Sr. This limit is based on the assumption that an isomeric transition or states fed directly by the β decay of the isomer would be seen in the γ spectra.

The measured K/L, $L_I/(L_{II}+L_{III})$, and K/M ratios for the 42.3-keV transition are also listed in Table V, and the theoretical predictions for various multipolarities[13] are listed in Table VII. The K internal-conversion coefficient α_K has also been obtained with the orange spectrometer by comparison with that obtained for the 381.5-keV transitions and is in good agreement with the $M2$ multipolarity indicated by the above results. The K/M ratio is also in good agreement with the recent calculation of Bhalla for a pure $M2$ transition.[14] The knowledge of this multipolarity was found to be an essential element in the decay scheme construction because of the strength of the transition and its location in the scheme.

The measured value of the transition energy was determined with the $\pi\sqrt{2}$ electron spectrometer as 42.3 ±0.05 keV.

TABLE VI. Electron binding energies, demonstrating that the 42.3-keV photon is a transition in rubidium.[a]

Nucleus	$E_K-E_{L_I}$ (keV)	E_K-E_M (keV)
Sr	13.89	15.80
Rb	13.13	15.0

[a] Reference 19.

TABLE VII. Theoretical internal-conversion coefficients for 42.3-keV transition in rubidium, as a function of multipolarity.[a]

α_K				K/L				$L_I/(L_{II}+L_{III})$			
$E1$	$E2$	$M1$	$M2$	$E1$	$E2$	$M1$	$M2$	$E1$	$E2$	$M1$	$M2$
1.06	16.2	1.52	32.9	9	3.2	8.6	5.6	3.4	0.36	13.4	3.4

[a] Reference 13.

[13] M. E. Rose, *Internal Conversion Coefficients* (Interscience Publishers, Inc., New York, 1958).
[14] C. P. Bhalla (private communication).

2. 762.5-keV Transition

The absolute conversion-coefficient measurements can be performed very satisfactorily by making an absolute measurement of a single transition, then comparing electron and photon relative intensities of the remaining transitions. The 762.5-keV K-conversion line, shown in Fig. 14, has been chosen as the standard line, and its absolute α_K measured via the mixed source technique. The internal-conversion line of the 661.6-keV transition in ^{137m}Ba has been used in conjunction with relative photon intensity measurements performed with a 7-cm^3 Ge(Li) detector having 4.5-keV resolution (full width at half-maximum). The relation

$$\alpha_K(762.5)=\alpha_K(661.6)\frac{I_e(762.5)}{I_e(661.6)}\frac{I_\gamma(661.6)}{I_\gamma(762.5)},$$

with the measured quantity[15] $\alpha_K(661.6)=0.0894$, yields the desired result directly.

As shown in Table VIII, the measured value of $\alpha_K=(9.5\pm0.5)\times10^{-4}$ for the 762.5-keV transition in ^{83}Rb agrees well with that expected for a pure $E2$ transition. However, an appreciable $M1$ admixture cannot be excluded. The K/L ratio, although not a very sensitive test of the multipolarity in this case, was unattain-

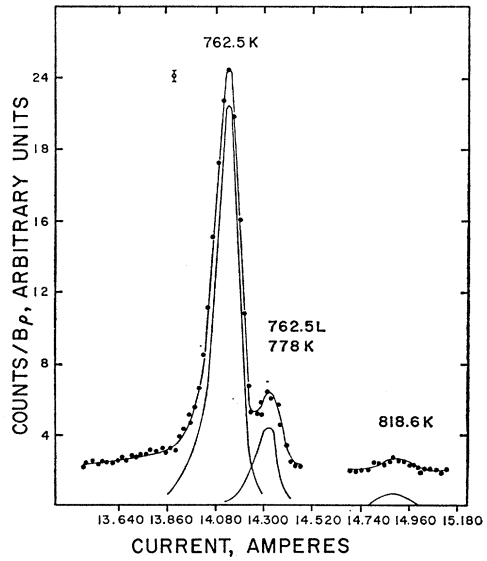

FIG. 14. The internal-conversion electron spectrum of ^{83}Sr, spanning the 740–830-keV region, recorded with the "orange" spectrometer.

[15] J. S. Merritt and J. G. V. Taylor, Anal. Chem. **37**, 351 (1965); Nucl. Sci. Abstr. **19**, No. 16860 (1965).

TABLE VIII. Multipole order of transitions in ^{83}Rb, based on measured values of the internal-conversion coefficients.

E_γ (keV)	Relative electron intensity $I_{(762K)}\equiv 100$	Relative γ-ray intensity $I_{(762\gamma)}\equiv 100$	α_K[a] (expt)	α_K[a] (theoretical) $E1$	$E2$	$M1$	$K/(L+M)$ (expt)	K/L (theoretical) $E1$	$E2$	$M1$	Multipole order
94.2	K 230	1.0	2.2±0.2(−1)	1.0(−1)	1.0(0)	1.5(−1)			6.5	8.7	$M1$, ≤10%$E2$
290.2	K 21; $L+M$ 2.1	1.4	1.4±0.2(−2)	3.9(−3)	1.8(−2)	7.9(−3)	10±2		8.6	9.0	35%$M1$, 65%$E2$
381.5[b]	K 440; $L+M$ 60	23.5; 36.5 → 60.0[c]	7.1±0.3(−3)	1.9(−3)	7.2(−3)	4.1(−3)	7.4	9.6	8.9	9.2	$E2$, <10%$M1$[b]
389.2	K 27; $L+M$ 3.2	4.0	6.5±0.5(−3)	1.8(−3)	6.7(−3)	3.9(−3)	8±2				$E2$, 20%$M1$
418.6	K 26	17.8	1.4±0.2(−3)	1.5(−3)	5.3(−3)	3.3(−3)					$E1$
423.5	K 7.8	4.6	1.6±0.4(−3)	1.4(−3)	5.1(−3)	3.2(−3)					$E1$
438.2	K 7.7	2.7	2.7±0.4(−3)	1.3(−3)	4.6(−3)	2.9(−3)					$M1$
762.5	K 100	100	9.5±0.5(−4)	3.6(−4)	9.3(−4)	8.8(−4)		8.7	9.3		$E2$(+$M1$)
778.4	K 5.5	5.5	9.6±2 (−4)	3.4(−4)	8.8(−4)	7.9(−4)					$M1$, $E2$
818.6	K 2.7	2.4	1.1±0.4(−3)	3.1(−4)	7.8(−4)	7.0(−4)					$M1$, $E2$

[a] The number in parentheses are the appropriate powers of 10, i.e., 2.2±0.2(−1) means (2.2±0.2)×10^{-1}.
[b] The 381.5-keV transition is a doublet, as described in Sec. 3B.
[c] The division of intensities of the 381.5-keV doublet are based on the coincidence results described in Sec. 3B.

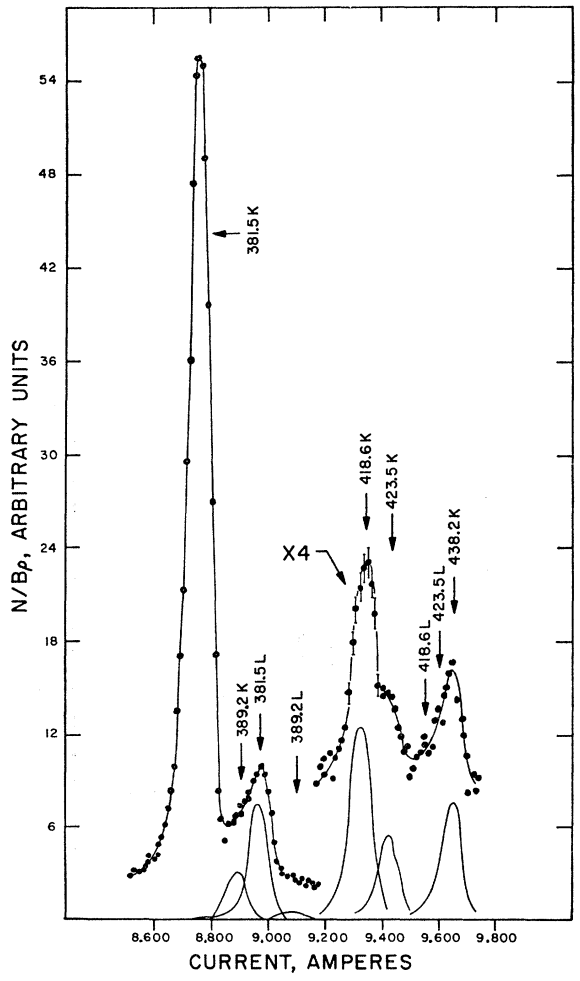

FIG. 15. The internal-conversion electron spectrum of ^{83}Sr spanning the 350–440-keV region. This was recorded with the "orange" spectrometer.

able because of the incomplete resolution of the 762.5-keV L and the 778.4-keV K lines in the internal-conversion spectrum.

3. 381.5-keV Transitions

The conversion electron spectrum encompassing the region from 350 to 440 keV is shown in Fig. 15. The peak corresponding to a 381.5-keV transition has been shown in Sec. 3B to be a cascading doublet on the basis of coincidence results, the upper member having about 60% of the intensity of the lower one. Thus, the α_K obtained for this peak must be considered as composite and was determined independently by both the mixed source technique and by comparison with the 762.5-keV α_K measurement described above. The former yields the result $\alpha_K=(7.2\pm0.3)\times10^{-3}$. Assigning $\alpha_K=9.5\times10^{-4}$ for the 762.5-keV transition, the value $\alpha_K=(7.0\pm0.3)\times10^{-3}$ was obtained for the composite peak when comparing relative electron and photon intensities. A simple average has been taken as the final value. Both values are in good agreement with the 7.2×10^{-3} theoretical $E2$ value,[13] as shown in Table VIII. Within the limits of the data, either both of the 381.5-keV transitions are $E2$ with an upper limit of 10% $M1$ or, if one is pure $E2$, the other transition may be mixed.

The measured $K/(L+M)$ ratio of 7.4±0.5 for the 381.5-keV transitions has been obtained by the standard stripping process, whereby counts from the unresolved 389-keV K line were removed. The theoretical K/L ratio[13] for an $E2$ transition is 8.9. Application of the semiempirical method of Chu and Perlman[16] to the M shell yields a value of 1.7×10^{-4} for the total M conversion coefficient. However, it has been shown[17] that the ratio of $M_{\text{Chu}}/M_{\text{exp}}$ may be as much as 1.7 in this

[16] Y. Y. Chu and M. L. Perlman, Phys. Rev. **135**, B319 (1964).
[17] O. Dragoun and P. Johns, Phys. Letters **24B**, 146 (1967).

mass region. Even if this is the case for this transition, the measured $K/(L+M)$ ratio can be considered to be in agreement with that expected for an $E2$ transition.

4. Remaining Internal-Conversion Coefficients

The K conversion lines corresponding to the 389.2-, 418.6-, 423.5-, and 438.2-keV transitions have been analyzed as shown in Fig. 15, using standard stripping techniques. The results of the analyses and the assigned multipolarities are given in Table VIII. The K conversion line of the 381.5-keV transitions was used for the standard line shape. The 438.2-keV K line is not completely resolved from the 418.6- and 423.5-keV L lines. However, the theoretical K/L ratio of 10 for these latter two transitions indicates that the majority of the intensity of this line arises from the 438.2-keV K conversion line.

Figure 16 shows the K conversion line of the 94.2-keV transition and the K and L lines of the 290.2-keV transition. A summary of the results and assigned multipolarities are also given in Table VIII. The 94.2-keV transition is not strong enough to allow a reliable K/L measurement, although a lower limit of 8 can be derived from the data.

The conversion electron spectrum from 740 to 870 keV is shown in Fig. 14. The intensity of the 778.4-keV electron line was obtained by subtracting from the total counts in the 762.5-L and 778.4-K composite line, an amount for the 762.5-keV L line based on the assumption that it is a pure $E2$ transition. The resulting α_K, listed in Table VIII, for the 778.4-keV transition, indicates an $M1+E2$ mixture, but little can be said about the mixing ratio within the experimental accuracy of the measurement.

5. Positron Spectra

The positron spectra have been measured with the orange spectrometer. The detector slit was opened wide to produce a higher positron count rate relative to counts registered from positrons annihilating in the material surrounding the detector. Under these circumstances the resolution was 2%.

The analysis of the Fermi-Kurie plot is shown in Fig. 17 and indicates branches with end-point energies at 1227±8, 803±15, and 465±50 keV. The stripping procedure was accomplished by making successive first-order least-squares fits to the high-energy fraction of the Fermi-Kurie plots. The resulting analysis indicates that there are 84.7, 9.2, and 6.1% of the positrons contained in the high-, intermediate-, and low-energy groups, respectively.

4. PROPOSED DECAY SCHEME

A decay scheme consistent with all our data has been constructed from the results of the coincidence studies, energy sums, and relative intensities of the transitions.

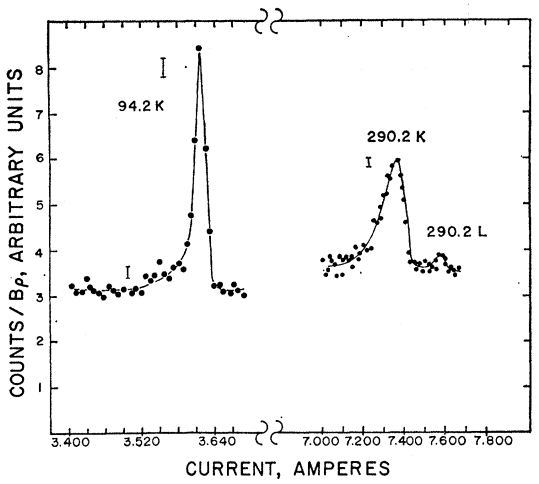

FIG. 16. The internal-conversion lines of 94.2- and 290.2-keV transitions in the decay of ^{83}Sr. Different sources were used for the two lines. The 290.2-K conversion line was recorded using a source thick enough to cause line broadening. These were recorded with the "orange" spectrometer.

This scheme is shown in Fig. 18. In general, a comparison of the energy sums of competing cascades and crossover transitions shows agreements to better than 0.5 keV for sums involving transitions having relative intensities greater than 0.5 (relative to 100 for the 762.5-keV transition) and usually to better than 1.0 keV for those involving the weaker photons.

The logft values listed in the decay scheme were determined from the relative intensities into and out of each state and from the x-ray and positron intensities. The positron branching ratios were determined from the Fermi-Kurie plots of the positron spectrum and from the triple coincidence experiments. The positron end points given in the decay scheme were obtained by assuming the 1227-keV branch is to the ground state and subtracting the state energies from this value. Explicit searches were made for positron feeding to the 736.8-keV state in triple-coincidence experiments with the positron annihilation radiation. No such feeding was found.

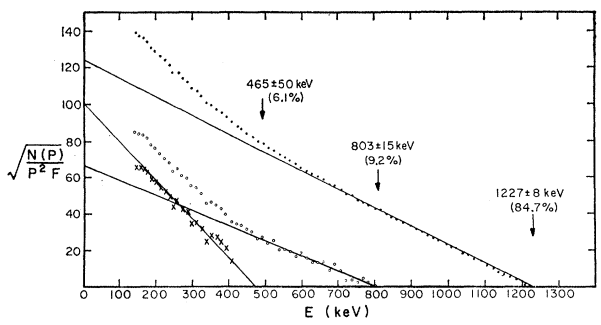

FIG. 17. The Fermi-Kurie analysis of the positrons emitted in the decay of ^{83}Sr. These data were recorded with the "orange" spectrometer.

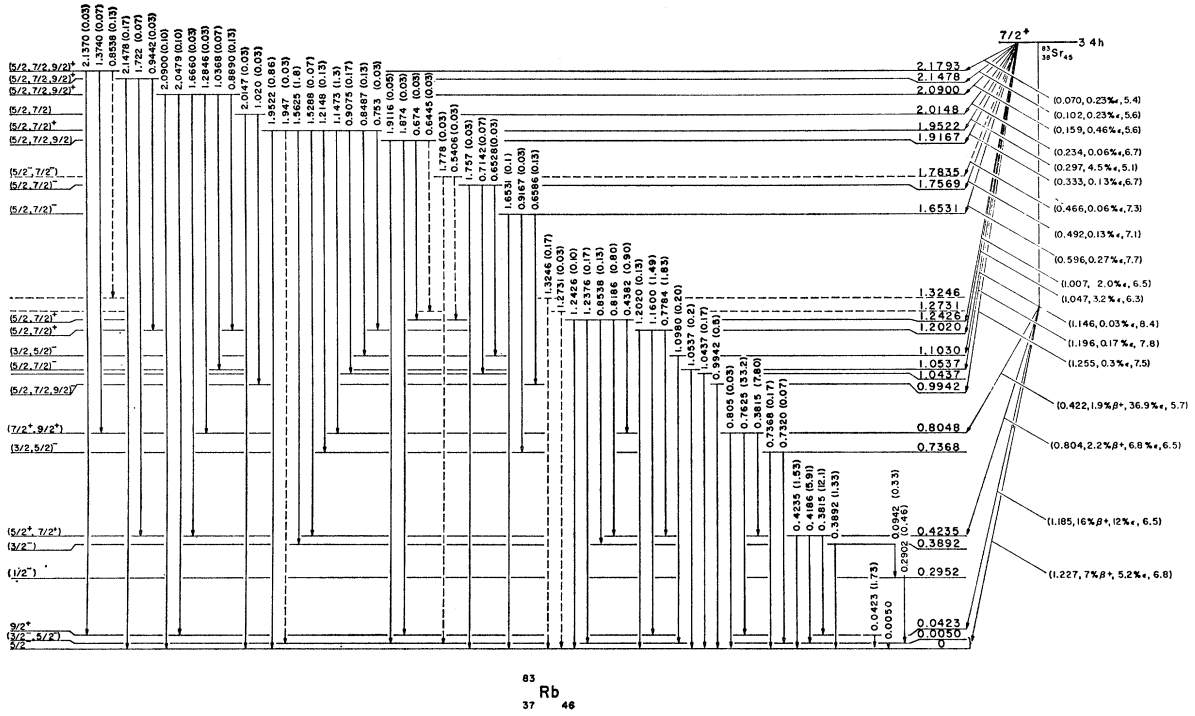

FIG. 18. The proposed decay scheme for ^{83}Sr. Energies are in MeV. The relative intensities given for the photons are in the units of percent per decay of the ^{83}Sr parent.

A. Evidence for the 42.3-keV State

The placement of a state at 42.3 keV was dictated by the relative intensity of the 42.3-keV transition and its long lifetime. The total internal-conversion coefficient has been measured to be 33, which gives a total of 188 units for this transition (relative to 100 for the 762.5-keV photon), making the 42.3-keV transition the strongest in the decay scheme.

B. Evidence for the 423.5-, 804.8-, and 5.0-keV States

A state was placed at 423.5 keV as a result of the relationships of the 381.5- and 423.5-keV photons in the coincidence spectrum. It is supported by several observed coincidence cascades that are listed in Table IV.

It was not possible to account for the relative intensity of the 42.3-keV transition without having the 762.5-keV photon feeding the 42.3-keV state. Furthermore, a very low intensity photon of about 805 keV was observed in the anti-Compton spectrum described in Sec. 3A. Therefore, a state was placed at 804.8 keV, which is the energy sum of the 42.3- and 762.5-keV transitions.

The 381.5-keV peak was shown in Sec. 3B to consist of two γ rays very close in energy and in coincidence with each other. The second 381.5-keV γ ray is therefore placed as depopulating the 804.8-keV state to the 423.5-keV state.

At this point, it was not possible to complete the construction of the decay scheme in a way that is consistent with the coincidence data without postulating the existence of a state at 5.0 keV. The previously mentioned intensity ratios of the 418.6- and 423.5-keV doublet imply that these transitions originate from the same state. In addition, there are other doublets with 5-keV energy differences, namely, the 732.0–736.8-, 1237.6–1242.6-, and 1947–1952.2-keV pairs. The 732.0–736.8-keV doublet also always occurred together and in the same intensity ratio in both singles and the coincidence spectra.

An effort was made to detect photons at 5.0-keV with a proportional counter and with a thin-window, high-resolution Si(Li) detector; but, because of the highly converted nature of low-energy transitions and the large background caused by the other photons and positrons, the results were inconclusive.

A careful search was made in both the photon and internal-conversion spectra for a transition of 37 keV which would fit between the 42.3- and 5.0-keV states. An upper limit of 1% can be placed on the intensity for such a 37-keV transition relative to the intensity of the 42.3-keV photon.

The triple-coincidence spectra (Fig. 12) support the placement of the states at 423.5 and 804.8 keV. Only the 381.5-, 418.6-, 423.5-, and 762.5-keV transitions are seen to be in prompt coincidence with the positrons. The positron branching ratios calculated from early

triple-coincidence data obtained from NaI(Tl) detectors were, in units relative to the 762.5-keV photons, 4.0±0.8 for the 804.8-keV state and 7.2±1.5 for the 423.5-keV state. These agree, to within the experimental error, with those obtained from the Fermi-Kurie plots, which were 5.2±1.0 for the 804.8-keV state and 7.9±1.5 for the 423.5-keV state. These values are consistent with those calculated using the proposed decay scheme and relative photon intensities and theoretical K/β^+ and E_K/E_L ratios.[18,19]

C. Evidence for States at 295.2 and 389.2 keV

The coincidence spectra show that the 1562.5-keV photon is in coincidence with the 94.2-, 290.2-, and 389.2-keV transitions and that the 94.2-keV photon is in coincidence with the 290.2-keV photon. The 389.2-keV photon was not observed to be in coincidence with either the 94.2- or 290.2-keV photons. The energy difference of 4.8 keV between the 389.2±0.5-keV and the sum of the 94.2±0.5- and the 290.2±0.5-keV photons is too large to be accounted for by the experimental errors of the energy measurements of these three photons; therefore the 389.2-keV photon cannot be a crossover transition for just the 94.2- and 290.2-keV photons alone. These coincidence data can be explained easily with the inclusion of the unobserved 5.0-keV transition in cascade with the 94.2- and 290.2-keV photons. Hence, states were placed at 295.2 and 389.2 keV.

The evidence for the placement of the state at 295.2 keV instead of at 99.2 keV is very weak. [*Note added in proof.* In a preliminary report, S. Morinobu *et al.*[20] presented data obtained from experiments similar to those reported herein. Their data are in substantial agreement with ours. They have also measured the half-life of the 42.3-keV state to be 7.8±0.7 msec., which is in agreement with the $M2$ assignment to the 42.3-keV transition. In a delayed-coincidence experiment on the 290–94-keV cascade, they found the half-life of the 94-keV transition to be 1.2 nsec. This establishes the order of the 290–94-keV cascade, which was found to be ambiguous in our experiments. This order is opposite to that given in the decay scheme shown in Fig. 18. S. Morinobu *et al.*[20,21] have also performed angular correlation experiments on the 1562–94-, 1562–290-, 1562–389-, and 1147–762-keV cascades. Their correlation coefficients are consistent with our spin assignments to the states involving these transitions.] The intensities of the 94.2- and 290.2-keV transitions are equal to within the experimental errors. According to the energy sum and relative intensities, the very weak 1796-keV transition fits nicely between the states at 2090.2 and 295.2 keV. However, the 1796-keV photon was seen only once and then in an anticoincidence spectrum that was taken over a very long time. Therefore, this transition is not placed in the scheme.

D. Evidence for States at 1202.0, 1242.6, and 1952.2 keV

The anti-Compton and the "any γ-γ" coincidence spectra indicate that the 1160.0-, 1202.0-, 1237.6-, 1242.6-, 1947-, and 1952.2-keV transitions are not in prompt coincidence with any other photons and therefore they probably populate the 42.3, 5.0 keV, or ground state. Numerous coincidence relationships and energy sums support the placement of states at 1202.0, 1242.6, and 1952.2 keV.

E. Remaining States

The remaining states account for a very small fraction of the decays of ^{83}Sr and were placed on the basis of the coincidence data and, in a few cases, upon the existence of an energy sum alone. Those transitions not observed in coincidence and not satisfying an energy sum were left out of the decay scheme. These were the 1296.0-, 1384.3-, 1596-, 1710-, 1749-, and 1796-keV photons.

5. SPIN AND PARITY ASSIGNMENTS

A. 42.3-keV State

The ground-state spin and parity of ^{83}Rb have been determined[22,23] by atomic-beam methods to be $\frac{5}{2}^-$. Since it was shown in Sec. 3C1 that the 42.3-keV transition has multipolarity $M2$, the spin and parity of the state at this energy is limited to $\frac{1}{2}^+$ or $\frac{9}{2}^+$. Although the $\frac{1}{2}^+$ assignment was considered, it did not lead to a consistent interpretation of all the data. On the other hand, the $\frac{9}{2}^+$ assignment, which might be expected on the basis of shell-model systematics, does lead to consistency. Hence, we tentatively assign spin and parity of $\frac{9}{2}^+$ to the 42.3-keV state.

B. 5.0- and 423.5-keV States of ^{83}Rb and the Ground State of ^{83}Sr

The 423.5-keV state decays via an $E1$ transition (423.5 keV) to the $\frac{5}{2}^-$ ground state, and by an $E2$ ($+M1$?) transition (381.5 keV) to the $\frac{9}{2}^+$ 42.3-keV state. Hence, the 423.5-keV state must have spin and parity $\frac{5}{2}^+$ or $\frac{7}{2}^+$. Any $M1$ admixture in the 381.5-keV transition would limit the choice to $\frac{7}{2}^+$.

From shell-model considerations and the systematics of the odd-A strontium isotopes, it is expected that

[18] M. L. Perlman and M. Wolfsberg, Brookhaven National Laboratory Report No. BNL 485(T-110), 1958 (unpublished).
[19] A. H. Wapstra, G. J. Nijgh, and R. Van Lieshout, *Nuclear Spectroscopy Tables* (North-Holland Publishing Co., Amsterdam, 1959), p. 58.
[20] S. Morinobu, I. Katayama, H. Adachi, M. Ishii, and H. Ikegami, Contributions to International Conference on Nuclear Structure, 1967, Tokyo, Japan, contribution No. 4.124, p. 169 (unpublished).
[21] S. Morinobu (private communication).
[22] J. B. Hobson, J. C. Hubbs, W. A. Nierenberg, H. B. Silsbee, and R. J. Sunderland, Phys. Rev. **104**, 101 (1956).
[23] J. C. Hubbs, W. A. Nierenberg, H. A. Shugart, H. S. Silsbee, and R. J. Sunderland, Phys. Rev. **107**, 723 (1957).

^{83}Sr will have spin and parity of $\frac{1}{2}^-$, $\frac{7}{2}^+$ or $\frac{9}{2}^+$. The logft values for the β transitions to the 42.3- and 423.5-keV states appear to be allowed, or possibly first forbidden. Hence, the spin and parity of $\frac{1}{2}^-$ is ruled out for the ground state of ^{83}Sr.

The $E1$ character of the 418.6-keV transition between the 423.5- and 5.0-keV levels implies the latter has negative parity with spin $\frac{3}{2}$ or greater, but less than $\frac{9}{2}$. As previously noted, an upper limit of 1% on the intensity of a 37.3-keV photon relative to that of the 42.3-keV photon has been set. If the 5-keV state had spin and parity of $\frac{7}{2}^-$ or $\frac{9}{2}^-$, this would suggest that an $E1$ transition between the 42.3- and 5.0-keV states would be retarded by a factor of 10^{11}, assuming that both it and the 42.3-keV $M2$ transitions were single particle. Furthermore, such an upper limit for the relative intensity of a 37.3-keV photon relative to that of the 42.3-keV photon would seem to rule out the possibility of an $M2$ transition between the states in question. Hence, we conclude that the spin and parity for the 5-keV state is $\frac{3}{2}^-$ or $\frac{5}{2}^-$, with the $\frac{3}{2}^-$ assignment being preferred. This then fixes the spin and parity of the 423.5-keV state as $\frac{5}{2}^+$, and from the logft value of 5.7 for the decay to this level, the ground state of ^{83}Sr is inferred as $\frac{7}{2}^+$.

C. 295.2- and 389.2-keV States

The $M1+E2$ character of the 290.2-keV transition, in conjunction with the spin and parity of the 5-keV state, establishes the parity of the 295.2-keV state as negative with spin $\frac{1}{2}$, $\frac{3}{2}$, or $\frac{5}{2}$. Of these possibilities, $\frac{5}{2}$ would be excluded by the high logft value (i.e., ≥ 9) for the decay to this level. Moreover, the absence of a transition from the 295.2-keV state to the $\frac{5}{2}^-$ ground state, as well as the absence of other transitions to this level (except for the 94.2-keV transition), would make a $\frac{3}{2}^-$ assignment difficult to comprehend. This, with the lower limit for the logft value for decay to this level, leads us to suggest spin and parity of $\frac{1}{2}^-$ for the 295.2-keV state.

The measured and assigned spins and parities for the ground and 295.2-keV states, respectively, in conjunction with the $E2$ and $M1+E2$ transitions from the 389.2-keV state to these levels, then determine the spin and parity of the 389.2-keV state as $\frac{3}{2}^-$. This assignment would be consistent with the logft value (i.e., >8) for the decay to this state.

D. 804.8-keV State

The $E2$ character of the transitions from the 804.8-keV state to the 42.3- and 423.5-keV states restricts the spin and parity to $\frac{5}{2}^+$, $\frac{7}{2}^+$, or $\frac{9}{2}^+$. These are consistent with the allowed logft value for the β decay to this level. From the absence of observed transitions to levels with spins $\frac{1}{2}$ and $\frac{3}{2}$, it would appear that $\frac{7}{2}^+$ or $\frac{9}{2}^+$ is most probable for the 804.8-keV state. Any $M1$ admixture in the 381.5-keV transition to the $\frac{5}{2}^+$ 423.5-keV state would eliminate the possiblity of $\frac{9}{2}^+$.

E. 1202.0-keV State

The $M1+E2$ character of the 778.4-keV transition, in conjunction with the allowed logft value for the β decay to the 1202.0-keV state, would restrict its spin and parity to $\frac{5}{2}^+$ or $\frac{7}{2}^+$. The fact that this level is observed to decay only to states with spins and parities of $\frac{5}{2}\pm$ and $\frac{9}{2}^+$ suggests that the spin and parity of the 1202.0-keV state is $\frac{7}{2}^+$.

F. 1242.6-keV State

The $M1$ character of the 818.6-keV transition, in conjunction with the allowed logft value for the capture decay to the 1242.6-keV level, would restrict its spin and parity to $\frac{5}{2}^+$ or $\frac{7}{2}^+$. The γ-ray branching from this level would seem to favor the $\frac{5}{2}^+$ assignment.

G. 1952.2-keV State

The logft value of 5.1 for the capture decay to the 1952.2-keV state implies that it should have spin and parity $\frac{5}{2}$, $\frac{7}{2}$, or $\frac{9}{2}^+$. Of these, the γ-ray branchings to levels with spins and parities of $\frac{3}{2}^-$, $\frac{5}{2}^-$, $\frac{5}{2}^+$, and $\frac{7}{2}^+$ would tend to favor a $\frac{5}{2}^+$ assignment to the 1952.2-keV state.

H. 2090.0-keV State

Here also the logft value of 5.6 would imply $\frac{5}{2}$, $\frac{7}{2}$, or $\frac{9}{2}^+$ for the spin and parity of the 2090.0-keV state. The photon branchings to levels with spins and parities $\frac{5}{2}^-$, $\frac{5}{2}^+$, $\frac{7}{2}^+$, and $\frac{9}{2}^+$ would seem to favor a $\frac{7}{2}^+$ assignment.

I. 2179.2-keV State

The allowed logft value and the observation of only γ-ray branches to levels with spins and parities $\frac{7}{2}^+$ and $\frac{9}{2}^+$ would seem to favor a $\frac{9}{2}^+$ assignment for the 2179.2-keV state.

6. DISCUSSION

The calculations of Talmi and Unna[1] predict the ground state of $_{38}{}^{83}Sr_{45}$ as $\frac{9}{2}^+$, with excited states of spin-parity $\frac{1}{2}^-$ at 170 keV and $\frac{7}{2}^+$ at 320 keV. Even though the odd-mass strontium isotopes ^{85}Sr and ^{87}Sr have similar level structures, the other 45-neutron even Z nuclei ^{77}Ge, ^{79}Se, and ^{81}Kr have $\frac{7}{2}^+$ ground states.[24] The $\frac{7}{2}^+$ assignment for ^{83}Sr, which has been inferred from this study, is thus consistent with the systematics in this region. The state possibly corresponds to a $(p_{1/2})^{-2}$ $(g_{9/2})^{-3}{}_{7/2}$ shell-model configuration.

[24] *Nuclear Data Sheets*, compiled by K. Way *et al.* (U. S. Government Printing Office, National Academy of Sciences—National Research Council, Washington, D. C.).

Figure 19 compares the few known states below 525 keV in the odd-mass rubidium isotopes. In ^{83}Rb, the ground state $(\frac{5}{2}^-)$, the 5.0 $(\frac{3}{2}^-)$-, the 4.23 $(\frac{9}{2}^+)$-, and 295.2$(\frac{1}{2}^-)$-keV states probably arise from shell-model proton configurations $(f_{5/2})^{-1}$, $(p_{3/2})^{-1}$, $(g_{9/2})^1$, and $(p_{1/2})^1$, respectively. However, the extremely close spacing of these levels may indicate an appreciable amount of a more complex configuration mixing. The low-lying $\frac{3}{2}^-$ state is expected since the $(p_{3/2})^{-1}$ and $(f_{5/2})^{-1}$ configurations are in competition for the ground state of the rubidium isotopes,[24] the former apparently prevailing for ^{81}Rb and ^{87}Rb, the latter for ^{83}Rb and ^{85}Rb. The $\frac{9}{2}^+$ states in ^{81}Rb and ^{85}Rb probably correspond to the same type configuration assigned for ^{83}Rb. The $\frac{9}{2}^+-\frac{5}{2}^-$ energy-level separation is changing very rapidly in this series of nuclei, the $\frac{9}{2}^+$ state actually being the lower state in ^{81}Rb. This trend may suggest that the 2970-keV state in ^{87}Rb is $\frac{9}{2}^+$, an assignment which is consistent with the logft value of the β transition to the level.[24] Very little is known about the level schemes of these other odd-mass rubidium isotopes, suggesting the need for further investigations in this region before systematic trends of the single-particle levels can be established.

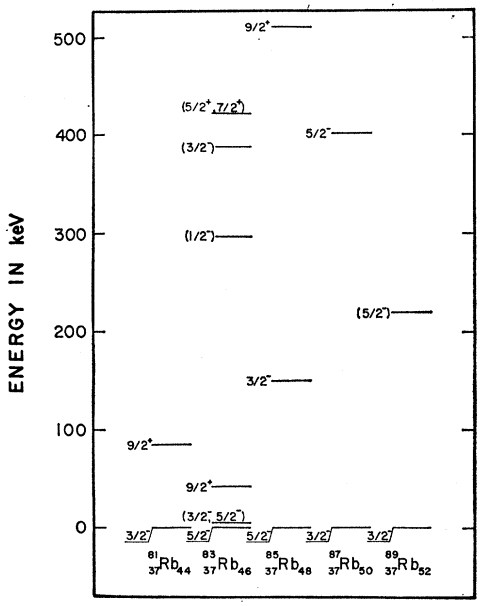

FIG. 19. Comparison of the low-energy levels of the odd-mass rubidium isotopes.

It is conceivable that some of the higher-energy states in ^{83}Rb could arise from more complicated shell-model configurations, as well as collective excitations. It is interesting to consider that the strongly excited 423.5- and 804.8-keV states can be attributed to the latter phenomenon. This can be done from two slightly different points of view, although there are objectionable features to both interpretations. First, it is noted that the 804.8-, 423.5-, and 42.3-keV states are connected by two relatively pure $E2$ transitions of comparable energy, hence suggestive of a vibrational structure built on the 42.3-keV $(\frac{9}{2}^+)$ single-particle state. The other point of view, based on the core coupling model of de-Shalit,[25] assumes the 804.8- $(\frac{7}{2}^+)$ and 423.5-keV $(\frac{5}{2}^+)$ states are part of a multiplet of states produced by coupling of the 2^+ core excitation with the $\frac{9}{2}^+$ particle state. However, transitions between members of the multiplet should be predominantly $M1$, whereas an upper limit of 40% can be placed on the $M1$ contribution of the observed transition. In either event, if the 804.8-keV state is truly of collective nature, the $E2$ transition probability of the 762.5-keV transition should be enhanced over the Weisskopf single-particle estimate.[19] A measurement of the lifetime of the state might serve to test the hypothesis.

Finally, one might expect similar collective states built on the ground and 5.0-keV states in much the same manner as they seem to be built on the $\frac{9}{2}^+$ state. The 389-keV level may have such a composition. However, most of the states formed in this manner may be inaccessible to the β-decay process, since it requires a $g_{9/2}$ neutron to be transformed into an $f_{5/2}$ or $p_{3/2}$ proton, a process which is both j- and l-forbidden. On the other hand, one might expect the decay of the $g_{9/2}$ extra core neutron in ^{83}Sr to very effectively populate levels built on the $g_{9/2}$ proton states in the ^{83}Rb daughter.

[25] A. de-Shalit, Phys. Rev. **122**, 1530 (1961).

ACKNOWLEDGMENTS

The authors wish to thank Dr. R. L. Auble and Dr. G. Berzins for assistance with the data analysis. We are also grateful to Dr. G. B. Beard for the use of his high-resolution Si(Li) detector. The assistance of Dr. W. P. Johnson and Dr. H. G. Blosser with the early MSU cyclotron runs is gratefully acknowledged. Two of the authors (W. H. K. and D. J. H.) wish to express their appreciation to the staff of the Lawrence Radiation Laboratory, Berkeley, Calif., for their splendid hospitality during the early stages of this investigation, and to the U. S. Atomic Energy Commission for its support during this same time. The aid of Dr. R. M. Diamond, of LRL, with the HILAC bombardments is very much appreciated. The encouragement and assistance of Dr. S. K. Haynes and W. C. Johnston with the measurements with the $\pi\sqrt{2}$ iron-free electron spectrometer are deeply appreciated. We wish to thank Dr. J. P. Hurley and J. M. Mathiesen for the use of their Ge(Li) detectors during the early stages of this work. One of the authors (R.C.E.) wishes to thank the NSF for the Science Faculty Fellowship that he held during the early stages of this investigation. Another of the authors (L.M.B.) wishes to gratefully acknowledge the assistance of an NDEA fellowship.